Reduction of the Influence of Intravenous Contrast in PET/CT by Using a Threshold Conversion Method

Catherine Lemmens, Johan Nuyts, Stijn Dirix and Sigrid Stroobants

***Abstract*— In PET/CT an attenuation map for PET is derived from the CT image. However, when a full diagnostic CT with intravenous contrast is performed, the PET attenuation values are overestimated. This results in increased SUV values when compared with contrast-free studies. Although several groups have reported that the impact of contrast on the SUV values is small, the effect may not be negligible in treatment follow-up. Conventionally the hybrid scaling method [1] is used for the conversion of CT attenuation values to PET attenuation. Here, we propose a new conversion method in an attempt to minimize the influence of the intravenous contrast on the SUV values. With the new method, CT attenuation values are converted from [0, 0.16] to [0, 0.091] (units in cm^{-1}) and all the attenuation values greater than the threshold 0.16 are converted to 0.091. The threshold value of 0.16 was derived using 9 patient studies involving 14 ROIs and was further evaluated using 5 patient studies involving 13 ROIs. For the first 9 patient studies, the mean influence of the intravenous contrast on the SUV values is 5.53% (range [1.59-11.63]) with the conventional method and 2.04% (range[0.25-5.73]) with the new threshold method. Very similar results were obtained in the second group: 5.90% (range [1.29-9.59]) with the conventional method and 1.91% (range [0.04-4.59]) with the new threshold method.**

I. Introduction

In recent years more and more conventional PET scanners are replaced by combined PET/CT systems [2]. PET/CT has several advantages over the conventional PET: PET/CT combines functional information with anatomical information and by performing two examinations in one scan, patients comfort is increased. Using the CT for attenuation correction gives an almost noise-free attenuation map and eliminates the need for a transmission scan thereby reducing the total examination time. By administering contrast agents, the CT image quality can be improved. However, these contrast agents cause an overestimation of the PET attenuation values resulting in increased SUV (Standardized Uptake Values). To eliminate the influence of the contrast agents on the SUVs, two CT scans can be performed: A low dose CT scan for attenuation correction and a diagnostic CT scan with intravenous (IV) contrast.

In our institution, the protocol used to examine follow-up patients isn't always the same. This causes a patient to have a low dose CT scan on one examination and a full diagnostic CT scan on another examination. Berthelsen et al. [3] and Yau et al. [4] have found that the effect of IV contrast on the SUV values is small and unlikely to affect the diagnosis. In [5], they found a significant increase in SUV due to IV contrast, but this increase was again clinically not significant. However, when PET is used to evaluate therapy response, the change in SUV caused by alternating the CT protocol may not be negligible [3], [4].

Our aim is to find a conversion method which gives rise to the same SUV values whether the low dose or the diagnostic CT scan is used for the attenuation correction of the PET. Such a conversion method eliminates the need for two CT scans and in follow-up, the most appropriate CT protocol can be selected without having an effect on diagnosis.

Other methods to reduce the artifacts caused by contrast agents were proposed: Laymon and Bowsher [6] use the PET emission data to identify whether high attenuation pixels are either correct or the result of improper contrast scaling. In [7] a region growing approach is used on a segmented image containing the high attenuation voxels. The algorithm extracts the largest connected region which corresponds to bone. The remaining voxels are identified as being contrast and are then replaced by water pixels. Lonn [8] uses a tissue contrast scaling for the reduction of the influence of the contrast. This scaling corresponds to a mixture model where each material is either a combination of air and water, or of water and contrast. This method improves the attenuation correction in the presence of IV contrast but also results in an underestimation of the attenuation values of bone. In [9], the most optimal protocol for IV contrast administration was searched which reduced both the contrast artifacts in CT as in PET.

Our approach is similar to the approach of Lonn, in the sense that we will also be adapting the conversion curve in order to reduce the influence of the contrast on the SUV values. Finding this new conversion method is considered as a two parameter optimization problem for which tradeoffs have to be made between bias and the influence of the IV contrast.

The traditional approach in PET/CT reconstruction is to start from the CT image and derive an attenuation map with reduced resolution. However, here we will first reduce the resolution of the raw CT data to that of the PET. This results in a strong reduction of the sinogram size, enabling the application of iterative reconstruction in a clinically acceptable processing time.

In the following, the reconstruction procedure is described and a new conversion method is proposed whereby the influence of IV contrast on the SUV values will be minimized.

The authors are with the Dept. of Nuclear Medicine, K.U.Leuven, B-3000 Leuven, Belgium. E-mail: catherine.lemmens@uz.kuleuven.be

This work was supported by the "Institute for the Promotion of Innovation through Science and Technology in Flanders (IWT-Vlaanderen)"

II. METHOD

A. CT reconstruction

The CT sinogram is resampled to the PET detector size and rebinned from fan beam to parallel beam configuration. The method is implemented for a dual slice CT and helical acquisition orbit: linear interpolation is used to produce sinograms for axial positions exactly matching that of the PET slices. The CT image is then reconstructed using a maximum-likelihood algorithm for transmission tomography (MLTR) [10], [11], using 100 iterations accelerated with subsets. The "raw" CT data obtained from the scanner have actually undergone several corrections, including the subtraction of a background from each detector reading, the crosstalk correction, off-focal radiation correction, beam hardening correction, the log-conversion, converting the measured intensities to the integrals of attenuation coefficients, azimuthal smoothing, and, in some scanners, ring removal.

The MLTR algorithm starts from a blank and a transmission sinogram, assuming that the blank sinogram is noise-free, while the transmission sinogram values are samples from a Poisson distribution. Although the real distribution is not exactly Poisson, the approximation is reasonable, and rightly assigns a lower signal-to-noise ratio to values corresponding to higher attenuation. In order to apply MLTR to the CT data, the "raw" CT data obtained from the scanner need to be converted back to measured intensities. For this an arbitrary noise-free blank scan of 10^5 photons per detector pixel is introduced. The transmission scan can then be calculated as $t_i = b_i \exp(-r_i)$, where b_i is the blank scan value for detector element i, r_i is the "raw" CT value and t_i is the computed transmission value.

The advantage of the MLTR reconstruction is that it is less prone to artifacts, in particular when metal objects are in the field of view [12] or when there is truncation of the CT projection [13]. Otherwise, the MLTR and the standard FBP (Filtered Back Projection) images are very similar.

B. Conversion to PET attenuation

After CT image reconstruction the CT values have to be converted to PET attenuation values. The current standard is the so called hybrid method [1], [14], which uses a piecewise linear scaling curve assuming each material is either a combination of air and water, or of water and bone (a mixture model). A similar approach has been proposed for SPECT [15]. However, the hybrid method is not optimized for all possible kVp settings available on a CT scanner [16]. Therefore, applying a kVp-dependent conversion gives rise to more correct PET attenuation values and thus improves tracer quantification.

The hybrid and the kVp-dependent conversion methods, which both make use of bilinear scaling curves, are effective in the absence of contrast agents. However, they produce an inappropriate scaling of contrast enhanced regions [17]. Contrast artifacts can be reduced by using the scaling of [16] for regions less dense than water and by setting the attenuation of denser regions to that of water. This will be called the 'clipping' method [12].

Analyzing CT images, we noticed that there is a significant amount of tissue having a density somewhat less than water. So, using the 'clipping' threshold method just described would not completely eliminate the effect of IV contrast. A further lowering of the threshold is desirable but this also introduces a negative bias in the final PET images. Therefore it would be opportune to adapt the linear scaling curve below the threshold value in order to reduce this bias.

Thus, finding the new conversion method comes down to optimizing the two parameters μ_p and μ_c as shown in fig. 1. Also shown in fig. 1 are the kVp-dependent scaling for 110 kVp and 130 kVp, the clipping method and the tissue contrast scaling of Lonn for 110 and 130 kVp. The threshold value μ_c

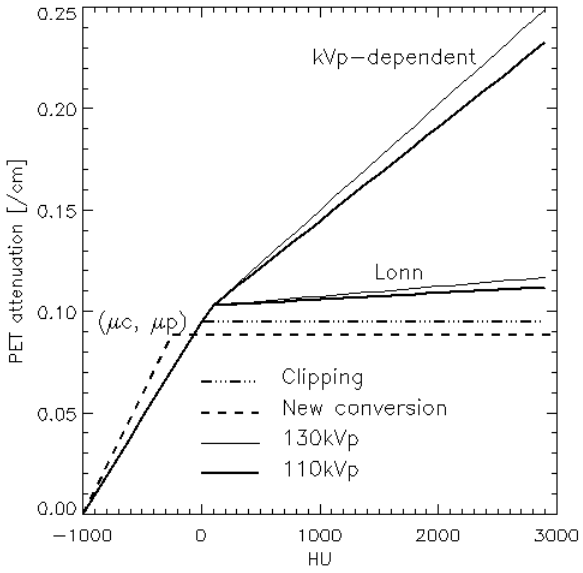

Fig. 1. Conversion from CT HU to PET attenuation.

must be chosen in such a way that it minimizes the influence of the IV contrast on the SUV values. The PET attenuation coefficient corresponding to μ_c in the kVp-dependent method will be increased to the value μ_p in order to reduce the bias. How the new conversion method, which we will call for the rest of this paper the 'threshold' method, was obtained will be discussed in section III and IV-A.

Finally, the resulting attenuation image is forward projected to produce the attenuation correction sinograms.

C. PET reconstruction

The 3D PET sinograms were corrected for detector sensitivity, dead time, scatter [18] and attenuation, and converted to 2D sinograms with Fourier rebinning [19]. For reconstruction, the sinograms were "uncorrected" for attenuation, and reconstructed with (attenuation weighted) MLEM, accelerated using a gradually decreasing number of subsets [20]. We verified that the resulting PET images were similar to the clinical images obtained with the commercial software.

III. PATIENT STUDIES

A. Data acquisition

Nine patient studies (Group1) were selected to search for the optimal values of μ_c and μ_p. Afterwards, another 5 studies

(Group2) were selected to evaluate the threshold conversion method. All patients were included in a phase II trial evaluating the efficacy of a histone deacetylase inhibitor. The imaging protocol for this project involved the acquisition of two whole body CT scans and one whole body PET scan. The radiotracer used was ^{18}F-FDG and patients were administered 5 MBq/kg ^{18}F-FDG with a maximum of 550 MBq.

All patients underwent first a low dose CT scan for attenuation correction. Immediately afterwards, the PET scan was acquired and thereafter a second, full diagnostic CT scan with IV contrast was performed. Patients were positioned supine with the arms placed above their head (if this was feasible for the patient). For the first CT scan and the PET scan, the groin till the top of the skull was imaged, whereas for the second CT, the groin till the lower jaws was imaged to reduce patient dose. The direction of the PET scans was caudocranial and of the CT scans it was craniocaudal. All PET/CT images were acquired on a Biograph system (Siemens), consisting of a dual slice CT system (Somatom Emotion) and a septaless LSO PET camera (Ecat Accel). The PET acquisition was done with 4 minutes per bed position, with typically 7 bed positions per study. The CT data were acquired with a slice thickness of 5 mm, using a 12 mm table feed per rotation, with a rotation time of 0.8 s. Low dose CT scans were acquired at 40 mAs and 110 kVp, full diagnostic CT scans were acquired at 85 mAs and 130 kVp. The scans were acquired during shallow breathing of the patients, with no breath holding instructions during the CT acquisition of the lung data. All patients received oral contrast (24 ml Telebrix, 300 mg iodine per ml, dissolved in 750 ml water). The IV contrast (120 ml Visipaque, 300 mg iodine per ml) was administered automatically with an injection speed of 1.6 ml/s. The time delay between the start of the injection of IV contrast and the second CT scan was 90 s.

B. Data reconstruction

For each patient two CT images were reconstructed using the method described in section II-A: The low dose CT image without IV contrast, CT(-IV), and a diagnostic CT image with IV contrast, CT(+IV).

Our off-line reconstruction of the CT images produces images in linear attenuation values per cm (μ). In order to apply the kVp-dependent scaling [16], these images needed to be converted to Hounsfield Units (HU), using the following relation:

$$HU = \frac{\mu - \mu_{H_2O}}{\mu_{H_2O}}.1000$$

The kVp-dependent scaling was implemented through the function [16]:

$$\begin{aligned} \text{Below break point:} \quad \mu &= \; 9.5\ 10^{-5}.\ (HU + 1000)\ \text{cm}^{-1} \\ \text{Above break point:} \quad \mu &= \; a\ .\ (HU + 1000) + b\ \text{cm}^{-1} \end{aligned}$$

The kVp-dependent values for a, b and the breakpoint, specific for the Biograph2 system, can be found in table I. These values were obtained from Siemens and deviate from the values mentioned in [16].

All CT scanners are calibrated so that 0 HU corresponds to the linear attenuation value of water μ_{H_2O}. As we did not know the effective energy of the Emotion 2 scanner, μ_{H_2O} could not be calculated. Therefore a scan with a water phantom was performed at each possible kVp of our Biograph 2 scanner. Off-line reconstruction of these images with the MLTR algorithm gave rise to a μ_{H_2O} of 0.1913 cm^{-1}. The calculated μ_{H_2O} was the same for all kVp, as was expected from the calibration of the scanner.

kVp	a (10^{-5} cm^{-1})	b (10^{-2} cm^{-1})	Break point (HU+1000)
110	4.63	5.21	1070
130	5.21	4.57	1065

TABLE I

THE KVP-DEPENDENT VALUES OF a, b AND THE BREAKPOINT FOR THE BIOGRAPH 2 SYSTEM.

The obtained CT images were then converted to PET attenuation maps using different conversion methods: The kVp-dependent method [16], the clipping method [12], the tissue contrast scaling of Lonn [8], and the threshold method. The kVp-dependent method was used as the standard conversion method with which all other methods were compared. For the threshold method, the threshold μ_c was varied between 0.18 cm^{-1} (-59 HU), which is somewhat below the threshold value for the clipping method (0.1913 cm^{-1} or 0 HU), and 0.15 cm^{-1} (-216 HU). For each threshold value μ_c, the corresponding PET coefficient μ_p was varied between 0.086 cm^{-1} and 0.094 cm^{-1}. For each of these conversion methods, PET images were reconstructed.

For the analysis of the PET images, 3-dimensional ROIs (Region Of Interest) were delineated by the physicians, using software based on thresholding and region growing [21]. Each ROI was defined on the PET image reconstructed with the attenuation map derived from the low dose CT, PET(-IV), using the kVp-dependent conversion method. The same set of ROIs were then applied to PET(-IV) and PET(+IV) for the analysis of all the conversion methods. For each conversion method, the mean SUV values were calculated for each ROI. The SUV values of the PET images reconstructed with the attenuation map derived from the low dose CT, PET(-IV), were compared with the SUV values of the PET images reconstructed with the attenuation map derived from the diagnostic CT, PET(IV+). The absolute and the relative differences for each method were calculated. Also the relative difference in SUV of PET(IV+) with respect to the standard PET image was calculated. The standard PET image is the image reconstructed with the attenuation map derived from the low dose CT scan and with the kVp-dependent conversion method.

C. Criteria for the new conversion method

A few criteria were formulated to assess the quality of the conversion method for the treatment evaluation based on PET/CT with variable CT protocol. The criteria were made based on the following quantities.

For each conversion method, the influence of the IV contrast on the SUV values will differ. To assess this influence, the relative difference in SUV is calculated for each ROI:

$$D_{mr} = \frac{|SUV(+IV)_{mr} - SUV(-IV)_{mr}|}{(SUV(+IV)_{mr} + SUV(-IV)_{mr})/2} * 100$$

with the m pointing at a specific conversion method and the r pointing at a ROI. The mean relative difference over all ROIs will be denoted by D_m.

To quantify the bias in the SUVs introduced by the different methods, the relative difference between the method and the standard kVp-dependent method is calculated for both CT scans:

$$A_{mr} = \frac{SUV(-IV)_{mr} - SUV(-IV)_{hr}}{SUV(-IV)_{hr}} * 100$$

$$B_{mr} = \frac{SUV(+IV)_{mr} - SUV(-IV)_{hr}}{SUV(-IV)_{hr}} * 100$$

with the subscript h pointing at the kVp-dependent method and m at the considered conversion method. The mean bias for any method is denoted by A_m and B_m. For each conversion method the root mean square (RMS) of the bias for CT(+IV) is also calculated:

$$E_m = \sqrt{\frac{1}{R}\sum_r B_{mr}^2}$$

where R is the total number of ROIs.

Based on these quantities, the following criteria were made to select the values μ_c and μ_p.

1) The influence of the IV contrast with the threshold method, D_t, must be as small as possible without violating constraints 2, 3 and 4.
2) The absolute value of the bias with the threshold method, $|B_t|$, must be smaller than the bias with the kVp-dependent method, B_h.
3) The RMS of the bias with the threshold method, E_t, must be smaller than the RMS with the kVp-dependent method.
4) The absolute value of the bias of PET(-IV) with the threshold method, $|A_t|$, must be smaller than B_h.

IV. Results

A. Group1

In group1, eighteen ROIs were defined. Table II [1] gives the tumor location and the results for each of these tumors. Analyzing the results for the kVp-dependent conversion method, a decrease of the SUV values in PET(+IV) was seen with respect to PET(-IV) for four ROIs (ROI 4, 5, 8 and 10), although an increase was expected. These decreases seemed to be the consequence of two things: First, large movements of bowel gasses between the two CT scans, see fig. 2, caused an underestimation of the attenuation and secondly, because a shallow breathing protocol was used, the lungs were probably scanned during different moments of the breathing cycle causing a discrepancy of attenuation coefficients between the two CT scans. In the further analysis we exclude these four ROIs.

[1]For the calculation of the SUV values and all quantities we used more significant numbers than stated here. This may cause some small inconsistencies when the quantities are recalculated based on the given values.

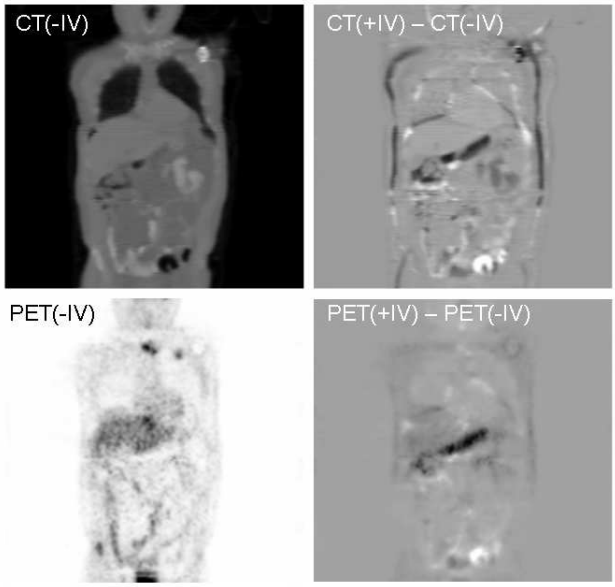

Fig. 2. Coronal slices of the CT without IV contrast and the corresponding PET scan are shown at the left. The top right panel shows the difference between the two CT scans (with and without IV contrast) and the lower right panel is the difference between the corresponding PET images.

Figures 3 through 6 show the results for the biases B_m and A_m, the RMS of the bias B_m and the influence of the contrast D_m as a function of the parameters μ_c and μ_p.

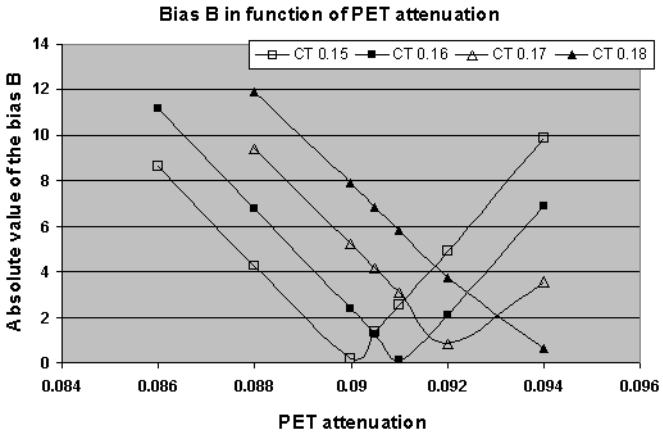

Fig. 3. The absolute value of the mean bias B_m as a function of the PET attenuation values μ_p (in cm^{-1}) when the CT attenuation value μ_c is kept constant at the values 0.15, 0.16, 0.17 and 0.18 cm^{-1}.

In these figures, the CT attenuation value μ_c was fixed at a certain value while the PET attenuation value μ_p was varied. When using the bias B_m (fig. 3) or A_m (fig. 4) as the criterion, the optimum value for μ_p increases with increasing μ_c. This can also be stated for the RMS of the bias E_m (fig. 5), but here better E_m values are obtained for the higher values of μ_c. For the CT attenuation value μ_c of 0.15 cm^{-1}, the value of the minimum is 6.79 %. This is above the RMS of the bias E_h of the kVp-dependent method, which is 6.62 %, so that a threshold value μ_c of 0.15 cm^{-1} or lower can be excluded.

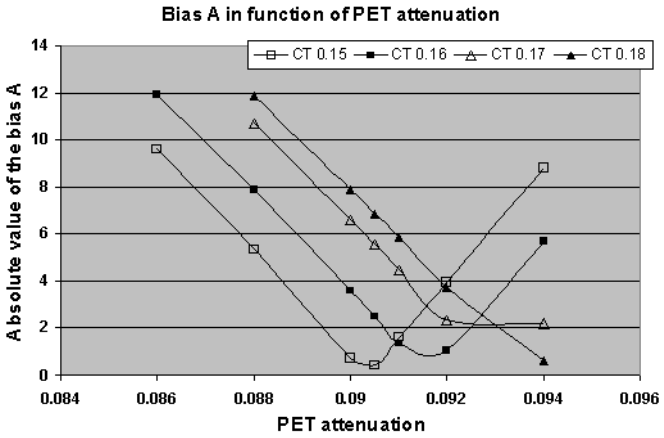

Fig. 4. The absolute value of the mean bias A_m as a function of the PET attenuation values μ_p (in cm^{-1}) when the CT attenuation value μ_c is kept constant at the values 0.15, 0.16, 0.17 and 0.18 cm^{-1}.

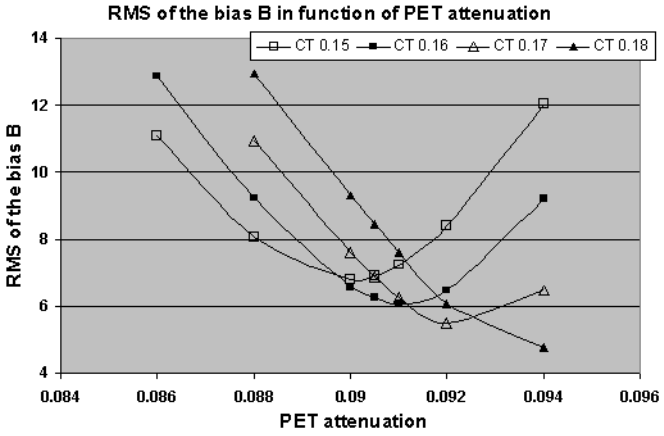

Fig. 5. The root mean square of the bias E_m as a function of the PET attenuation values μ_p (in cm^{-1}) when the CT attenuation value μ_c is kept constant at the values 0.15, 0.16, 0.17 and 0.18 cm^{-1}.

The general trend in fig. 6 is that the influence of the contrast D_m decreases with decreasing μ_c and μ_p.

Comparing the results for all combinations of parameters μ_c and μ_p, a threshold of 0.16 cm^{-1} (-164 HU), which is converted to the PET attenuation value of 0.091 cm^{-1}, seems to be the best choice. Since for μ_c, the CT value 0.15 cm^{-1} was already excluded based on the criterion for the RMS of the bias, 0.16 cm^{-1} is the value that will reduce the influence of the IV contrast the most. If μ_c is 0.16 cm^{-1}, the biases A_t and B_t, and the RMS of the bias E_t will be minimized when the PET attenuation value μ_p is chosen equal to 0.091 cm^{-1}.

The mean relative difference D_m between SUV(-IV) and SUV(+IV) for the kVp-dependent method is 5.53 %. With the tissue contrast scaling this difference is 5.24 %, with the clipping method it is 3.01 %, and with the threshold method the influence of the contrast is further reduced to 2.04 %. The standard deviation on these values are respectively 3.21 %, 3.15 %, 2.45 % and 1.36 %. Criterion 1 on D_t is thus fulfilled.

The use of the diagnostic CT for attenuation correction gives rise to a bias in the SUV values. With the kVp-dependent

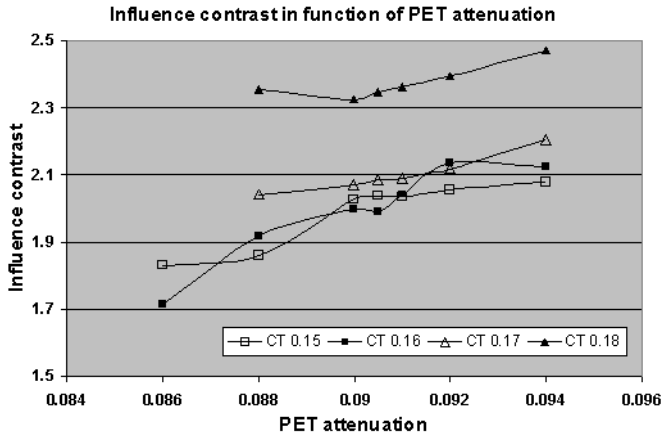

Fig. 6. The influence of the contrast D_m as a function of the PET attenuation values μ_p (in cm^{-1}) when the CT attenuation value μ_c is kept constant at the values 0.15, 0.16, 0.17 and 0.18 cm^{-1}.

method the mean bias B_h is 5.74 %. The use of the diagnostic CT and the tissue contrast scaling results in a bias B_l of 4.72 %. For the clipping and the threshold method these biases are respectively -2.07 % and -0.17 %. The E_m values are respectively 6.62 %, 5.80 %, 4.28 % and 6.08 %. Criteria 2 and 3 are thus fulfilled. As can be seen in fig. 5, the RMS of the bias can be further reduced by taking a higher value for μ_c (and by also increasing the corresponding μ_p). However, as the main goal of this paper is to suppress the influence of the IV contrast D_m as much as possible, we do not prefer to increase μ_c as this would augment D_m. If one is interested in the best bias results, the clipping method is to be preferred.

The use of the low dose CT scan for attenuation correction also gives rise to a bias in the SUV values when the kVp-dependent method is not used for conversion. For the tissue contrast scaling, the clipping and the threshold method, A_m is respectively -0.67 %, -4.80 % and -1.32 %, so criterion 4 is also fulfilled.

B. Group2

In the second group of patients, thirteen ROIs were drawn. The location of each of these tumors and the results for the kVp-dependent, the clipping, the tissue contrast and the threshold method are shown in table III. The mean results can be found in table IV.

With this group of patients, we wanted to check the reproducibility of the threshold method. The mean relative difference between SUV(-IV) and SUV(+IV) for the kVp-dependent method is 5.90 $\pm$ 2.34 % in this group. For the tissue contrast, the clipping and the threshold method D_m is respectively 5.76 $\pm$ 2.30 %, 3.24 $\pm$ 1.93 % and 1.91 $\pm$ 1.61 %. These results are in accordance with the results obtained for group1.

Regarding the bias, B_m is 6.11 % for the kVp-dependent method, 5.16 % for the tissue contrast method, -3.28 % for the clipping method and -4.06 % for the threshold method. The RMS of the bias E_m is respectively 6.56 %, 5.76 %, 4.67 % and 7.19 %. For the tissue contrast, the clipping and

Group1		kVp-dependent conversion				Clipping conversion		Tissue Contrast conversion		Threshold conversion	
Tumor nr	Location	SUV -IV	SUV +IV	D_{hr}	Bias B_{hr}	SUV D_{cr}	Bias B_{cr}	SUV D_{lr}	Bias B_{lr}	SUV D_{tr}	Bias B_{tr}
1	Liver	5.64	6.01	6.31	6.51	1.12	-3.47	6.24	6.00	0.25	-4.92
2	Liver	5.46	5.94	8.45	8.83	1.65	-4.66	8.34	7.92	1.35	-7.38
3	Breast	3.31	3.38	1.86	1.88	1.64	1.09	1.80	1.86	0.88	6.38
4	Breast	3.71	3.55								
5	Liver	3.52	3.24								
6	Lung	3.53	3.71	4.84	4.96	4.43	1.16	4.81	4.04	2.97	10.53
7	Lung	3.68	3.75	1.73	1.75	0.45	-4.67	1.27	0.82	2.21	-0.91
8	Adrenal	4.92	4.84								
9	Liver	4.18	4.26	1.99	2.01	1.16	-5.32	1.64	1.47	2.19	-4.59
10	Lung	4.60	4.49								
11	Lung	3.35	3.76	11.63	12.34	8.08	4.42	11.01	11.07	5.73	7.73
12	Adrenal	5.51	6.14	10.75	11.36	7.81	6.02	10.49	10.91	2.64	8.55
13	Lung	6.37	6.68	4.76	4.88	2.26	-3.10	4.02	3.29	1.41	-2.15
14	Lung	4.04	4.26	5.32	5.46	3.77	-3.79	4.76	2.87	2.39	-1.1
15	Lung	9.59	10.32	7.29	7.57	3.95	-0.55	6.61	6.57	2.57	3.62
16	Lung	3.42	3.60	5.05	5.18	1.93	-4.62	4.83	4.52	0.93	-6.06
17	Lung	8.31	8.81	5.88	6.06	3.41	-4.5	5.84	5.07	2.45	-4.76
18	Lung	8.34	8.47	1.59	1.61	0.46	-7.07	1.61	-0.34	0.61	-7.37

TABLE II

RESULTS FOR THE FIRST GROUP. FOR EACH ROI THE TUMOR LOCATION IS GIVEN EVEN AS THE SUV VALUES OBTAINED WITH THE STANDARD KVP-DEPENDENT METHOD. THE INFLUENCE OF THE CONTRAST, D_{mr}, AND THE BIAS, B_{mr}, ARE GIVEN FOR EACH ROI FOR THE KVP-DEPENDENT, THE CLIPPING, THE TISSUE CONTRAST AND THE THRESHOLD METHOD

Group2		kVp-dependent conversion				Clipping conversion		Tissue Contrast conversion		Threshold conversion	
Tumor nr	Location	SUV -IV	SUV +IV	D_{hr}	Bias B_{hr}	SUV D_{cr}	Bias B_{cr}	SUV D_{lr}	Bias B_{lr}	SUV D_{tr}	Bias B_{tr}
19	Liver	10.71	11.25	4.95	5.07	1.30	-7.04	4.75	4.20	0.04	-11.57
20	Kidney	8.69	9.26	6.31	6.52	4.16	0.03	6.43	6.00	0.80	-0.76
21	Liver	8.73	9.55	9.01	9.43	4.47	-3.75	8.44	8.27	2.47	-8.62
22	Kidney	6.67	7.23	8.01	8.34	5.27	0.70	7.93	7.68	1.06	-0.64
23	Liver	5.17	5.70	9.59	10.07	4.46	-3.01	9.45	9.79	4.23	-7.45
24	Bone	4.37	4.68	6.76	7.00	5.75	-5.53	6.64	4.21	4.59	-7.00
25	Liver	5.66	5.92	4.48	4.58	0.63	-11.35	4.22	4.15	0.89	-17.29
26	Peritoneum	3.79	4.01	5.62	5.78	2.59	-1.26	5.63	5.61	2.12	-3.08
27	Subcutaneous	3.49	3.68	5.40	5.55	2.53	-4.08	4.81	4.06	1.34	0.49
28	Lung	11.27	12.16	7.62	7.92	6.01	1.36	7.74	7.27	4.25	4.66
29	Axillary LN	9.94	10.15	2.16	2.18	0.89	-3.62	2.17	1.05	0.44	-2.90
30	Lung	10.46	10.99	4.90	5.03	3.25	-0.93	4.74	4.13	2.51	3.16
31	Axillary LN	9.28	9.46	1.92	1.93	0.87	-4.15	1.94	0.71	0.08	-3.28

TABLE III

RESULTS FOR THE SECOND GROUP. FOR EACH ROI THE TUMOR LOCATION IS GIVEN EVEN AS THE SUV VALUES OBTAINED WITH THE STANDARD HYBRID METHOD. THE INFLUENCE OF THE CONTRAST, D_{mr}, AND THE BIAS, B_{mr}, ARE GIVEN FOR EACH ROI FOR THE KVP-DEPENDENT, THE CLIPPING, THE TISSUE CONTRAST AND THE THRESHOLD METHOD

the threshold method, A_m is respectively -0.75 %, -6.30 % and -5.69 %. For the threshold method, the bias is somewhat worse compared to group1. This can be explained by the fact that group2 contains more tumors in the abdomen as discussed

		Group1	Group2	Abdomen	Lung
kVp-dependent	D_h	5.53	5.90	6.85	4.80
	B_h	5.74	6.11	7.12	4.95
	E_h	6.62	6.56	7.55	5.70
Clipping	D_c	3.01	3.24	3.36	2.93
	A_c	-4.80	-6.30	-6.19	-4.99
	B_c	-2.07	-3.28	-3.22	-2.19
	E_c	4.28	4.67	5.26	3.73
Tissue Contrast	D_l	5.24	5.76	6.68	4.53
	A_l	-0.67	-0.75	-0.55	-0.84
	B_l	4.72	5.16	6.35	3.80
	E_l	5.80	5.76	6.85	4.76
Threshold	D_t	2.04	1.91	1.89	2.05
	A_t	-1.32	-5.69	-6.31	-1.12
	B_t	-0.17	-4.06	-5.27	0.54
	E_t	6.08	7.19	8.14	5.14

TABLE IV

THE MEAN RELATIVE DIFFERENCE, THE RELATIVE BIAS AND THE RMS OF THE BIAS FOR THE KVP-DEPENDENT, THE CLIPPING, THE TISSUE CONTRAST AND THRESHOLD METHOD ARE GIVEN FOR EACH GROUP.

in the next section.

C. All patient studies

When considering all patient studies (Group1 and Group2), the ROIs can be divided in 2 groups according to their location: ROIs in the lungs and ROIs in the abdomen. The results in table IV show that for ROIs in the abdomen, D_h is higher than for ROIs in the lungs: 6.85 $\pm$ 2.45 % compared with 4.80 $\pm$ 2.75 % for the kVp-dependent method. SUV values for tumors located in the abdomen, are thus more affected by the IV contrast. The reason for this is that most abdomen tumors are surrounded with tissues having a high uptake of IV contrast whereas lung tumors are surrounded with tissues having a low uptake of IV contrast. For the threshold method, D_t for ROIs in the abdomen is 1.89 $\pm$ 1.45 % and 2.05 $\pm$ 1.51 % for ROIs in the lungs. The mean bias B_t for abdomen and lung ROIs is respectively -5.27 % and 0.54 %. A_t is respectively -6.31 % and -1.12 %.

In the lung ROIs there is less bias compared to the abdomen ROIs. This is due to the fact that in the chest, more tissue is in the range below the threshold value. Compared with the kVp-dependent method, these tissues have a higher attenuation value in the threshold method. E_t is 8.14 % for ROIs in the abdomen and 5.14 % for ROIs in the lungs. So in the abdomen, the threshold method reduces the influence of the contrast well but at the same time the RMS of the bias is increased.

The results are somewhat better for the lung group. This is probably due to the fact that the threshold method was optimized using group1, which contained a higher fraction of lung ROIs.

D. Bone region

In the tissue contrast, the clipping method and the threshold method the attenuation values of bone are set to lower values causing an undercorrection of the attenuation in the bone pixels. For many tracers, including ^{18}F-FDG, the uptake in bone is very low, so the undercorrection is not expected to produce noticeable artifacts. However, when a tumor is present in bone, one would expect this undercorrection to give rise to a high negative bias in the SUV values. Therefore, we took a closer look at ROI 24 which is a bone tumor located in the vertebra. All the results for this tumor can be found in table V. In the case of the low dose CT, the use of the clipping and the threshold method introduces a large negative bias A_m. However, when the diagnostic CT scan is used for attenuation correction, the biases B_{lr}, B_{cr} and B_{tr} are in absolute value smaller or equal to the bias B_{hr} due to the IV contrast in the case of the kVp-dependent method. So, when IV contrast is administered, the tissue contrast, the clipping method and the threshold method not only reduce the influence of the IV contrast but they also give better bias results. These results indicate that for this particular bone tumor, it would also be beneficial to use the threshold method in the case of follow-up.

	SUV(-IV)	SUV(+IV)	D_{mr}	A_{mr}	B_{mr}
kVp-dependent	4.37	4.68	6.76	0	7.00
Clipping	3.90	4.13	5.75	-10.8	-5.53
Tissue contrast	4.26	4.56	6.64	-2.48	4.21
Threshold	3.88	4.07	4.59	-11.2	-7.00

TABLE V

THE SUV VALUES AND THE QUANTITIES D_{mr}, A_{mr} AND B_{mr} ARE GIVEN FOR THE BONE TUMOR (ROI 24) FOR THE KVP-DEPENDENT, THE CLIPPING, THE TISSUE CONTRAST AND THE THRESHOLD METHOD.

V. DISCUSSION

For the kVp-dependent conversion method, a piecewise linear scaling curve is used which has the same slope for all kVps below $\sim$ 70 HU and a kVp-dependent slope above $\sim$ 70 HU. The clipping method uses the same scaling as the kVp-dependent method for tissues having a density lower than that of water (0 HU), and sets all tissues with a density higher than that of water to the attenuation value of water (0.095 cm^{-1}). The tissue contrast scaling corresponds to a mixture model where each material is either a combination of air and water, or of water and contrast.

As can be seen in table IV, the use of the tissue contrast or the clipping method already reduces the effect of the IV contrast on the SUV values. Although this reduction is small, it is important when PET is used as a surrogate marker of response in clinical trials. A reduction in FDG uptake of 15% after 1 cycle or 25% after 2 cycles is considered as a partial response [22]. Therefore the effect of the IV contrast cannot be considered negligible in this setting.

The analysis of CT images without IV contrast revealed that many tissues actually have a density somewhat below that of water. Therefore lowering the threshold value for clipping seems reasonable and will further reduce the variability due to IV contrast. However, this will also increase the negative bias. The 'threshold' method, converts the CT attenuation

values from [0, 0.16] cm^{-1} (or [-1000, -164] HU) to [0, 0.091] cm^{-1} and converts all the CT attenuation values higher than 0.16 cm^{-1} to the PET attenuation value of 0.091 cm^{-1}, as illustrated in fig. 7. By increasing the PET attenuation values

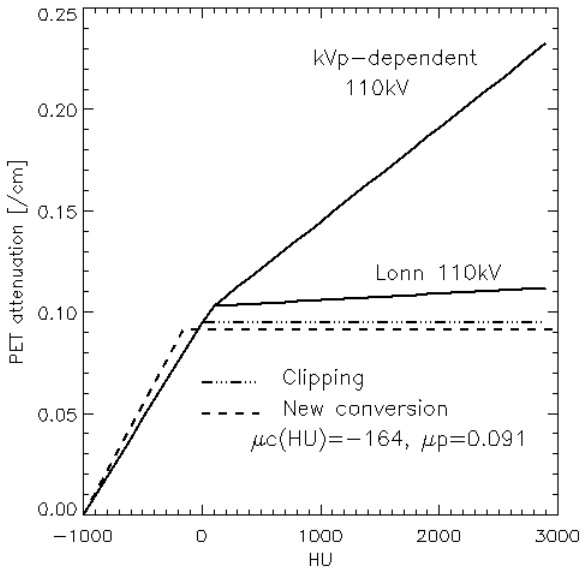

Fig. 7. Conversion from CT in HU to PET attenuation.

below 0.091 cm^{-1} with respect to the attenuation values in the kVp-dependent method, the negative bias is reduced.

Both the clipping and the threshold method reduce the variances at the cost of increased bias. In follow-up studies this may be beneficial, since there, systematic errors are less important because the analysis is focused on changes in tracer uptake. This is particularly true when the CT protocol is varied to reduce the radiation to the patient.

On the other hand, if both the absolute SUV value and the evaluation of the SUV over time are of interest, the clipping method is to be preferred as it gives the best bias results.

Recently, Berthelson et al. [3] performed a similar study on the effect of IV contrast on SUV values. For the conversion of the CT values to PET attenuation values, they used the hybrid method and the tissue contrast method of Lonn [8]. Their study demonstrated that a diagnostic CT scan with IV contrast can be used for attenuation correction of the PET data without changing the clinical diagnostic interpretation. However, for follow-up, they stated care has to be taken when a CT scan with IV contrast is used for attenuation correction. Another result, similar with ours, is that a different tracer uptake in PET(-IV) and PET(+IV) is not mainly due to IV contrast. Movement of bowel gasses in between the two CT scans leads to local under- and overestimation of the SUV values. Patient movement and breathing also cause changes in the SUV values, especially at the body surface and the borders of the lungs. As seen in our study the artifacts due to movement of bowel gasses and breathing can sometimes surpass the artifacts due to the IV contrast.

Dividing the ROIs of group1 and group2 into lung and abdomen ROIs, revealed differences between the two groups. These difference are the consequences of a different uptake of IV contrast in the surrounding tissues of lung tumors and abdomen tumors and of a difference in attenuation values of their surrounding.

The threshold method undercorrects the attenuation values of bone highly. This is expected to give rise to a large negative bias. However, the results for the particular bone tumor under consideration, show that even in follow-up it can still be beneficial to use the threshold method.

The traditional approach in PET/CT reconstruction is to reconstruct the CT image with FBP at a resolution of 512x512 and then down sample this image to derive the attenuation map for PET. Here, the reconstruction of the CT images was done by first down sampling the resolution of the raw CT data to that of PET resolution and then perform the CT reconstruction with MLTR. MLTR was preferred for CT reconstruction over FBP because MLTR produces less artifacts in the case of metals and truncation. First down sampling the data and then reconstructing the data has a negligible impact on the attenuation values (or HU) of the CT image. So, we believe that the results of this paper will also be valid in the case of the traditional approach for CT reconstruction.

VI. Conclusion

The diagnostic CT can be used for attenuation correction. In follow-up studies and clinical trials, where the focus is on changes in tracer uptake over time, the effect of IV contrast on the SUV values may not always be neglected. In our study, changes up to 12 % were observed. The threshold conversion method reduced these to a maximum of 5 %. Therefore it may be beneficial in these cases to apply the threshold conversion method in order to minimize the effect of the IV contrast on the SUV values. When using the threshold method, a bias is introduced in the SUV values. Thus if one wants to make conclusions based on the absolute SUV values, the clipping method is the preferred conversion method.

VII. Acknowledgement

The authors thank Michel Defrise and Xian Liu for the Fourier rebinning software, Christian Michel and Mérence Sibomana for scatter correction and file I/O software, Karl Stierstorfer and colleagues from Siemens for help with the CT file format, Albert Lonn for information on the Tissue Contrast scaling and David Faul for information on the Siemens kVp-dependent scaling methods.

References

[1] P. Kinahan, D. Townsend et al., "Attenuation correction for a combined 3D PET/CT scanner", *Med Phys*, vol. 25, 2046-2053, 1998.

[2] T. Beyer, D. Townsend et al., "A combined PET/CT scanner for clinical oncology", *J Nucl Med*, vol. 41 (8), 1369-1379, 2000.

[3] A. Berthelsen, S. Holm, A. Loft, T. Klausen, F. Anderson, L. Højgaard, "PET/CT with intravenous contrast can be used for PET attenuation correction in cancer patients", *Eur J Nucl Med Mol Imaging*, vol. 32, 1167-1175, 2005.

[4] Y.-Y. Yau, W.-S. Chan, Y.-M. Tam et al.,"Application of intravenous contrast in PET/CT: Does it really introduce significant attenuation correction error?", *J Nucl Med* vol. 46 (2), 283-291, 2005.

[5] O. Mawlawi, J. J. Erasmus, R. F. Munden, T. Pan et al.,"Quantifying the effect of IV contrast media on integrated PET/CT: Clinical evaluation", *Am J Roentgenol* vol. 186 (2), 308-319, 2006.

[6] C. Laymon and J. Bowsher, "A log likelihood based method for recovery of localized defects in PET attenuation-correction images", *IEEE NSS-MIC*, proceeding, 2004.

[7] J. Carney, T. Beyer, D. Brasse et al., "CT-based attenuation correction for PET/CT scanners in the presences of contrast agent", *IEEE NSS-MIC*, proceeding, 2002.

[8] A. Lonn, "Evaluation of method to minimize the effect of X-ray contrast in PET-CT attenuation correction", *IEEE NSS-MIC*, proceeding, 2003 (3), 2220-2221.

[9] T. Beyer, G. Antoch, A. Bockisch and J. Stattauss, "Optimized intravenous contrast administration for diagnostic whole-body ^{18}F-FDG PET/CT, *J Nucl Med*, vol. 46 (3), 429-435, 2005.

[10] J. Nuyts, B. De Man, P. Dupont, M. Defrise, P. Suetens and L. Mortelmans, "Iterative reconstruction for helical CT: a simulation study", *Phys Med Biol*, vol. 43, 729-737, 1998.

[11] B. De Man, J. Nuyts, P. Dupont et al., "Reduction of metal streak artifacts in x-ray computed tomography using a transmission maximum a posteriori algorithm", *IEEE Trans Nucl Sci*, vol. 47 (3), 977-981, 2000.

[12] J. Nuyts and S. Stroobants, "Reduction of attenuation correction artifacts in PET-CT", *IEEE NSS-MIC*, proceeding, 2005, 1895-1899.

[13] J. Carney, D.W. Townsend, P.E. Kinahan, et al., "CT-based attenuation correction: the effects of imaging with the arms in the field of view", *J Nucl Med*, vol. 42 (5), proceeding SNM 2001, no. 211.

[14] C. Burger, G. Goerres, S. Schoenes, et al., "PET attenuation coefficients from CT images: experimental evaluation of the transformation of CT into PET 511-keV attenuation coefficients", *Eur J Nucl Med*, vol. 29 (7), 922-927, 2002.

[15] S.C. Blankespoor, X. Wu, K. Kalki, et al.,"Attenuation Correction of SPECT Using X-Ray CT on an Emission-Transmission CT System: Myocardial Perfusion Assessment", *IEEE Trans Nucl Sci*, vol. 43 (4),2263-2274, 1996.

[16] J. P. J. Carney, D. Townsend, V. Rappoport and B. Bendriem, "Method for transforming CT images for attenuation correction in PET/CT imaging", *Med Phys*, vol. 33 (4), 976-983, 2006.

[17] S. Nehmeh, Y. Erdi, H. Kalaigian, et al., "Correction for oral contarst artiafcts in CT attenuation-corrected PET images obtained by combined PET/CT", *Eur J Nucl Med Mol Imaging*, vol. 44 (12), 1940-1944, 2003.

[18] C.C. Watson, "New, faster, image-based scatter correction for 3D PET", *IEEE Trans Nucl Sci*, vol. 47 (4), 1587-1594, 2000.

[19] M. Defrise, P. Kinahan, D. Townsend, C. Michel, M. Sibomana and D. Newport, "Exact and approximate rebinning algorithms for 3D PET data", *IEEE Trans Med Imaging*, vol. 16, 145-158, 1997.

[20] H. M. Hudson and R. S. Larkin, " Accelerated image reconstruction using ordered subsets of projection data", *IEEE Trans Med Imaging*, vol. 13 (4), 601-609, 1994.

[21] N. C. Krak, R. Boellaard, O. S. Hoekstra et al., "Effects of ROI definition and reconstruction method on quantitative outcome and applicability in a response monitoring trial", *Eur J Nucl Med Mol Imaging*, vol. 32, 294-301 and 1245, 2005.

[22] H. Young, R. Baum, U. Cremerius and et al., "Measurement of clinical and subclinical tumour response using [18F]-fluorodeoxyglucose and positron emission tomography: review and 1999 EORTC recommendations. European Organization for Research and Treatment of Cancer (EORTC) PET Study Group." *Eur J cancer*, vol. 35 (13), 1773-1782, 1999.